*Tellus (2003), 55B, 159–169*
*Printed in UK. All rights reserved*


**TELLUS**
*ISSN 0280–6509*

# Reconstruction of past variations of $\delta^{13}C$ in atmospheric $CO_2$ from its vertical distribution observed in the firn at Dome Fuji, Antarctica

By S. SUGAWARA[1]*, K. KAWAMURA[2]†, S. AOKI[2], T. NAKAZAWA[2] and G. HASHIDA[3], [1]*Institute of Earth Science, Miyagi University of Education, Sendai 980-0845, Japan;* [2]*Center for Atmospheric and Oceanic Studies, Tohoku University, Sendai 980-8578, Japan;* [3]*National Institute of Polar Research, Tokyo 173-8515, Japan*

(Manuscript received 23 January 2002; in final form 23 September 2002)

ABSTRACT

Temporal variations of $\delta^{13}C$ of atmospheric $CO_2$ in the past have been reconstructed from the $\delta^{13}C$ values of $CO_2$ observed in firn at Dome Fuji, Antarctica. The effective diffusivities of $CO_2$ in firn were estimated for Dome Fuji and another Antarctic site, H72. The age distributions of $^{13}CO_2$ in firn were first calculated by using a one-dimensional diffusion model, and then the past values of the atmospheric $\delta^{13}C$ were derived by using an iterative procedure so that the calculated and observed vertical profiles of $\delta^{13}C$ of $CO_2$ in firn agreed with each other. This reconstruction method was also applied to the $CH_4$ concentration to confirm its validity. The values of the atmospheric $\delta^{13}C$ thus estimated were in good agreement with those from direct atmospheric measurements at Syowa Station, Antarctica, even for the levelling off of the secular decrease observed in the first half of the 1990s. The statistical uncertainty of the iterative procedure was examined by adding normal pseudo-random numbers to the observed $\delta^{13}C$ values in firn. We also calculated the $\delta^{13}C$ values for firn at H72 using the reconstructed history of the atmospheric $\delta^{13}C$, and its vertical profile was found to be in close agreement with the observational result.

## 1. Introduction

The carbon isotopic ratio, $\delta^{13}C$, of atmospheric $CO_2$ is a powerful tool for evaluating the $CO_2$ exchange fluxes between the atmosphere and the oceans or the terrestrial biosphere, because the effect on the atmospheric $\delta^{13}C$ is different in these exchange processes (Siegenthaler and Münnich, 1981; Keeling et al., 1989). Its systematic observations for background air have been made at various ground-based sites, as well as on ships and aircraft (Friedli et al., 1987; Keeling et al., 1989; Francey et al., 1990; Nakazawa et al., 1993a, 1997; Trolier et al., 1996; Morimoto et al., 2000). However, long records of the atmospheric $\delta^{13}C$ covering the last few decades are quite limited.

The analysis of air collected from firn of polar ice sheets is one of the most promising methods for reconstructing temporal variations of atmospheric constituents in the past, because the firn air is older than the surface atmosphere due to diffusive gas transport in firn and due to firn air not diffusing in the lock-in zone (Schwander et al., 1988, 1993; Schwander, 1989). The concentration variations of atmospheric constituents at the surface of the ice sheet are gradually propagated downward in firn by molecular diffusion and by downward advection of firn layers. As a result, the concentration of secularly increasing constituents, such as $CO_2$, $CH_4$ and $N_2O$, decreases with increasing depth. The effect of the gravitational settling on those

*Corresponding author.
e-mail: sugawara@staff.miyakyo-u.ac.jp
†Present affiliation: Climate and Environmental Physics, University of Bern, Sidlerstrasse 5, CH-3012 Bern, Switzerland.

vertical concentration profiles is relatively small, because their concentration increases in the atmosphere were enhanced especially during the last few decades. On the other hand, the isotopic ratios of these constituents in firn are influenced strongly not only by the history of their changes in the atmosphere but also by the gravitational settling, because the isotopic enrichment is caused by the mass-dependent diffusion of species in firn column. Therefore, the reconstruction of past atmospheric variations of the isotopic ratio from its vertical profile in firn is much more complex than that of the concentration. However, Trudinger et al. (1997) tried to retrieve the histories of $\delta^{13}C$ of atmospheric $CO_2$ and $CH_4$ by applying the "diffusion correction" to the data from firn at Law Dome, Antarctica.

In this study, we developed a one-dimensional diffusion model to reconstruct the past $\delta^{13}C$ values of atmospheric $CO_2$ from its vertical profile in firn, and applied it to the data taken in firn at Dome Fuji, Antarctica. The validity of our analytical method was examined by comparing with the results from direct atmospheric measurements at Syowa Station, Antarctica. In addition, we also calculated the vertical profile of $\delta^{13}C$ for firn at an Antarctic site, H72, where the temperature and the accumulation rate are quite different from those at Dome Fuji, using the atmospheric $\delta^{13}C$ variations derived in this study, and compared it with the observational result.

## 2. Diffusion model

### 2.1. Model description

Our one-dimensional diffusion model was based on the theoretical formulation for the diffusion process by Schwander et al. (1993) and the bubble trapping process by Rommelaere et al. (1997). The theoretical basis and finite differential scheme of the model are as follows.

The basic process of air movement in firn was the same as proposed originally by Schwander et al. (1993) and used subsequently by Trudinger et al. (1997) and Rommelaere et al. (1997). It was assumed that the molecular diffusion flux in the open pore space arises from the concentration gradient and the gravitational effect

$$F = -D(z)\left[s\frac{\partial}{\partial z}\left(\frac{c}{s}\right) - \frac{mgc}{RT}\right]. \quad (1)$$

Here, $D$ denotes the diffusion coefficient of the trace gas molecule to be considered. This coefficient is not a pure molecular diffusion coefficient, but an effective value for the tortuous space in the firn layer. Therefore, it is called 'effective diffusivity' to distinguish from the pure diffusion coefficient. The variables $s$, $c$ and $T$ represent the open porosity, the trace gas concentration and the firn temperature, respectively. The constants $m$, $g$, and $R$ are the mass number of the trace gas, the acceleration of gravity, and the gas constant, respectively. The vertical advection flux of the trace gas, which is caused by air trapping at the close-off zone and downward bulk motion of firn, is also important, especially for sites with large accumulation rates. In previous studies, different mathematical expressions were used for this process. For example, Schwander et al. (1993) assumed a successive shifting down of discretely divided firn layers, while Trudinger et al. (1997) introduced the coordinate system which moves downward at the vertically dependent speed of firn. In this study, we adopted an expression given by Rommelaere et al. (1997). Mass conservation of the trace gas is given by

$$\frac{\partial c}{\partial t} + \frac{\partial (vc)}{\partial z} + \frac{\partial F}{\partial z} + rc = 0, \quad (2)$$

for the open pore space and

$$\frac{\partial c_b}{\partial t} + \frac{\partial (v_f c_b)}{\partial z} - rc = 0, \quad (3)$$

for bubbles. Here, $c$ and $c_b$ are the trace gas quantities in the open pore space and bubbles, respectively. The vertical speed of air in the open pore space, $v$, is distinguished from that of firn itself, $v_f$. At the transition zone where the open pore air is gradually trapped into bubbles, the mass conservation is given by using the bubble trapping rate, $r$ ($s^{-1}$). This simply means that a portion of the trace gas quantity in the open pore space, $rc$, is added to bubbles. A mathematical expression of the bubble trapping rate is given by Rommelaere et al. (1997) to be

$$r = -v_f \frac{s_t}{s}\frac{\partial}{\partial z}\left(\frac{s}{s_t}\right), \quad (4)$$

where $s_t$ is the total porosity. The total porosity was calculated from the firn density data using the equation

$$s_t = 1 - \frac{\rho}{\rho_{ice}}, \quad (5)$$

where $\rho$ and $\rho_{ice}$ are the densities of firn and ice (kg $m^{-3}$), respectively. At the transition zone, the total

porosity should be divided into the open and closed porosity. In this study, the closed porosity, $s_c$, was calculated by using the empirical equation given by Schwander (1989):

$$s_c = s_t \exp\left[75\left(\frac{\rho}{\rho_{close}} - 1\right)\right], \quad (6)$$

where $\rho_{close}$ is the density at the close-off depth. Under the steady state condition for firn densification, the vertical speed of firn, $v_f(z)$, is simply given by

$$v_f = \frac{a_s}{\rho}, \quad (7)$$

where $a_s$ is the accumulation rate (kg m$^{-2}$ s$^{-1}$). Equations (2) and (3) denote conservation of mass for the trace gas. However, the equations for the relative concentrations are preferable for more accurate calculation. The relative concentrations in the open pore space and bubbles, $x$ and $x_b$, are expressed by

$$x = \frac{c}{c_{air}} \text{ and } x_b = \frac{c_b}{c_{air,\,b}}, \quad (8)$$

respectively. Here, $c_{air}$ and $c_{air,b}$ are the air quantities (mol m$^{-3}$) for the open pore space and bubbles, respectively. The vertical profile of the air quantity in the open pore space was calculated from the barometric equation. The air quantity in bubbles, $c_{air,b}$, and the vertical advection speed of the open pore air, $v$, were determined by integrating the mass conservation equations for air in the closed and open pores, respectively.

To solve the differential eq. (2) numerically, the Crank–Nicolson method (Crank, 1975) was applied. In this method, implicit and explicit differentiations in the time domain were added with the same weight for the stable calculation. Thus, we obtain a tridiagonal system of discrete variable of the concentration, which can be easily solved by using the Thomas algorithm (Hirsch, 1988). On the other hand, the upwind differential method was applied to solve eq. (3). In this method, the stability of the numerical integration is controlled by the Courant number

$$\mu = v_f \frac{\Delta t}{\Delta z}, \quad (9)$$

and this should be less than 1 for the stable calculation. We set 1.0 d and 1.0 m for $\Delta t$ and $\Delta z$, respectively, so that the Courant number became sufficiently small, i.e. less than $10^{-3}$. In this connection, the vertical speed of firn, $v_f$, is less than about 11 cm yr$^{-1}$ at Dome Fuji and about 90 cm yr$^{-1}$ at H72, as seen in Fig. 1.

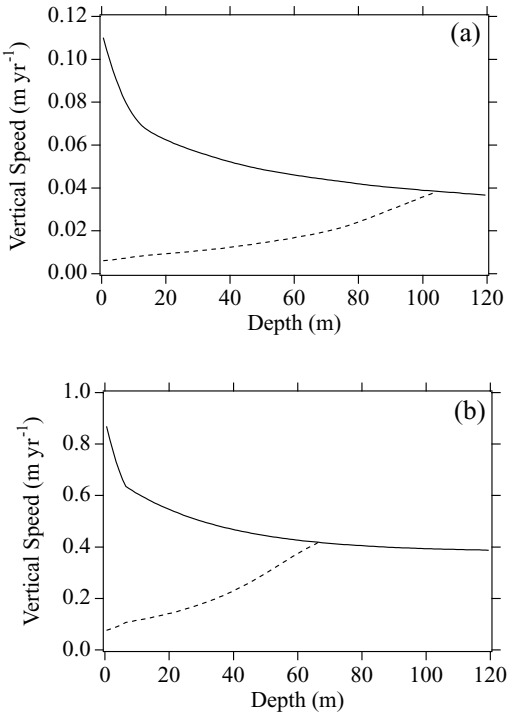


*Fig. 1.* Vertical speeds of firn (solid lines) and open pore air (dotted lines) at (a) Dome Fuji and (b) H72, calculated using the mass conservation equations.

As seen from Table 1, Dome Fuji is characterized by very low accumulation and temperature. Under such conditions, the bubble trapping at the close-off zone occurs slowly and the advection speed of air in the open pores is low. As shown in Fig. 1, the advection speed of the open pore air was calculated to be 3.8 cm yr$^{-1}$ at the close-off zone and less than 1.0 cm yr$^{-1}$ near the surface. This means that the vertical distributions of air components in open firn at Dome Fuji are controlled mainly by molecular diffusion. On the other hand, the air advection speed at H72 is larger by almost one order than that at Dome Fuji, which means that both the diffusive and advective transport processes are important for the H72 firn. Figure 2 shows the vertical profiles of the bubble trapping rate calculated using eq. (4) for the Dome Fuji and H72 firn. The bubble trapping rate increases from zero at the top of the close-off zone to the maximum at the bottom of the close-off zone. The maximum value amounts to about 0.05 and 0.7 yr$^{-1}$ for Dome Fuji and H72, respectively, which implies that 5 and 70% of air included in the 1 m thick firn

Table 1. *Geographical information of Dome Fuji and H72 and parameters used for model simulation*

| | Dome Fuji | H72 |
|---|---|---|
| Location | 77°19′S, 39°42′E | 69°12′S, 41°07′E |
| Elevation (m a.s.l.) | 3810 | 1241 |
| Sampling date | December 13–25 1998 | September 12–21 1998 |
| Accumulation (kg $m^{-2}$ $yr^{-1}$) | 32 | 350 |
| Surface density (kg $m^{-3}$) | 300 | 390 |
| Mean temperature (K) | 215 | 253 |
| Mean pressure (hPa) | 600 | 836 |

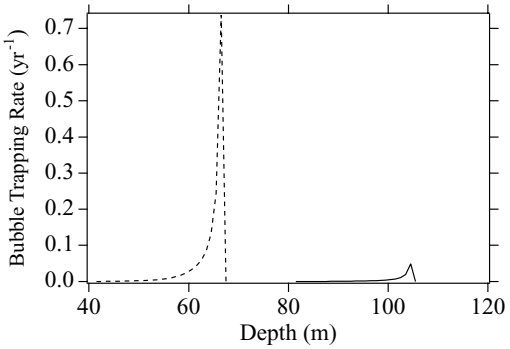


*Fig. 2.* Bubble trapping rate calculated for firn at Dome Fuji (solid line) and H72 (dotted line).

layer at the depths of maximum bubble trapping rate are occluded into bubbles every year. Thus, the loss term of the gas quantity in the open pore space, expressed by *rc* in eq. (2), is quite different for the two sites.

### 2.2. *Estimation of effective diffusivity*

In this study we derived the effective diffusivity of $CO_2$ by using an iterative procedure so that the vertical profile of the $CO_2$ concentration observed in firn was well reproduced. For this purpose, the time series of the $CO_2$ concentration for the past 273 yr was constructed on the basis of the data from the analyses of an Antarctic H15 ice core for 1725–1957 (Nakazawa et al., 1993b; Kawamura et al., 2000) and in situ measurements at the South Pole for 1957–1984 (Keeling et al., 1995) and Syowa Station for 1984–1998 (our unpublished data). An initial guess of the effective diffusivity of $CO_2$, $D_{\mathrm{init}}(z)$, was calculated by the equation

$$D_{\mathrm{init}}(z) = D_0 \left(\frac{T}{253}\right)^{1.85} \left(\frac{1013}{p}\right) [1.7s(z) - 0.2], \tag{10}$$

where $s(z)$ and $D_0$ represent the open porosity at a depth $z$, and the diffusion coefficient of $CO_2$ at 253 K and 1013 hPa, respectively. We set $1.247 \times 10^{-5}$ $m^2$ $s^{-1}$ for this parameter (Trudinger et al., 1997). The dependence of the effective diffusivity on the open porosity was based on the direct measurement of diffusivity for an Antarctic ice core, Siple (Schwander et al., 1988; Schwander, 1989).

Using the time series of the atmospheric $CO_2$ concentration and the initial guess of the effective diffusivity, the vertical distribution of the $CO_2$ concentration in firn was integrated from January 1725 to the date when the firn air were sampled at Dome Fuji. The vertical profile of the $CO_2$ concentration on the sampling date could be changed by employing the different effective diffusivities. Therefore, the sensitivity of the concentration profile to the effective diffusivity was first examined. If we define a variable $q_{jk}$ as a response of the $CO_2$ concentration at layer $j$ to a minimal change of the effective diffusivity given at layer $k$, it represents an element of a square matrix $\mathbf{Q}$. The differences between the calculated and observed $CO_2$ concentrations in firn can be expressed by a combination of the sensitivities weighted by the corrector vector $\phi$ under the linear approximation

$$x_{\mathrm{calc}} - x_{\mathrm{obs}} = \mathbf{Q}\phi. \tag{11}$$

Therefore, the initial guess of the effective diffusivity was corrected for its inadequacy by

$$D = D_{\mathrm{init}} + \mathbf{Q}^{-1}(x_{\mathrm{calc}} - x_{\mathrm{obs}}). \tag{12}$$

However, eq. (12) does not give good results when the calculated and observed $CO_2$ concentrations are

largely different, because the response of the calculated $CO_2$ concentration to the diffusivity is essentially non-linear. Therefore, the correction of the effective diffusivity was controlled by the optimum parameter $\kappa$,

$$D_{i+1} = D_i + \kappa \mathbf{Q}_i^{-1}(x_{\mathrm{calc},i} - x_{\mathrm{obs}}). \quad (13)$$

Here, suffix $i$ denotes the number of times of the iterative calculation. We empirically chose a sufficiently small value of 0.01 for the parameter $\kappa$. After correcting the effective diffusivity by eq. (13), the matrix $\mathbf{Q}$ was newly calculated using the revised effective diffusivity. These calculation procedures were repeated until the standard deviation of the concentration differences became smaller than 1 ppmv. In this iterative calculation, we simply constrained the effective diffusivity to decrease monotonously with increasing depth.

The profiles of the effective diffusivity obtained for the firn at Dome Fuji and H72 are shown in Fig. 3. At Dome Fuji, the effective diffusivity decreases slightly with increasing depth in the upper 20 m below the surface and then decreases steeply below. The effective diffusivity at H72 shows a steeper vertical gradient and becomes almost zero at 60 m. Since the close-off zone at H72 was estimated to be about 55–66 m from direct measurements of impermeability of the firn core, the lower half of the close-off zone, i.e. about 60–66 m, was thought to be the so-called 'non-diffusive layer' (Sowers et al., 1992). Such a layer was also found at GRIP, Greenland (Schwander et al., 1993), the South Pole (Battle et al., 1996), and DE08,

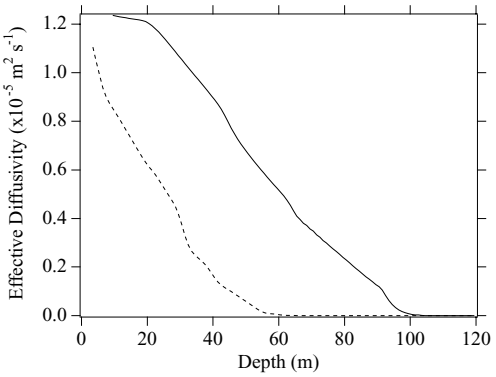


*Fig. 3.* Effective diffusivities of $CO_2$ in firn at Dome Fuji (solid line) and H72 (dotted line), estimated by using the vertical $CO_2$ concentration profile in firn and its atmospheric variation.

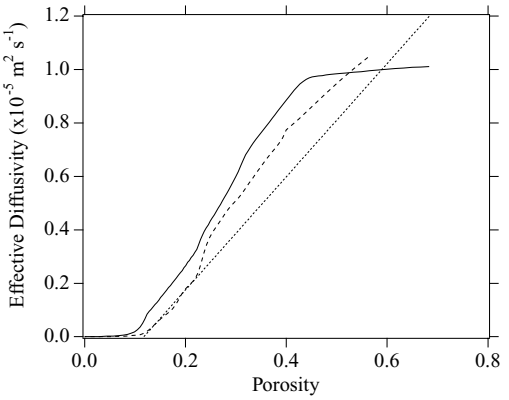


*Fig. 4.* Relationships between the effective diffusivity and the porosity estimated for firn at Dome Fuji (solid line) and H72 (dashed line). The linear relationship calculated using eq. (10) for Siple Station is also shown (dotted line). All the effective diffusivities were normalized to the values at 253 K and 1013 hPa.

Antarctica (Trudinger et al., 1997). The existence of the non-diffusive layer at H72 is also supported by the fact that $\delta^{15}$N of $N_2$ and $\delta^{18}$O of $O_2$ become constant in firn below 60 m (Kawamura, 2000).

The relationships between the open porosity and the effective diffusivity for Dome Fuji and H72, normalized at standard temperature and pressure, are shown in Fig. 4, together with the result calculated by using eq. (10). The three relationships are different, probably due to different firn structures at the respective locations. In general, the effective diffusivities estimated in this study are larger than that at Siple at the same porosity value. Rommelaere et al. (1997) also found that their effective diffusivities estimated for Vostok and DE08–2, Antarctica were larger by 25% than the results of the direct measurement at Siple. In addition, the profile of the effective diffusivity estimated for Vostok is quite similar to our result for Dome Fuji, except for the uppermost layer of firn. Considering that both locations are characterized by low temperatures, the above results suggest that the tortuousity of firn depends strongly on the firn structure, which is closely related to temperature.

## 3. Reconstruction of atmospheric $\delta^{13}$C

The value of $\delta^{13}$C in firn air is controlled mainly by its atmospheric variation history and the different diffusivities and the gravitational separation of two

isotopes. The thermal diffusion enhanced in the uppermost layer of firn is also a possible cause for the changes of the isotopic ratios. The thermal diffusion is expressed mathematically by the thermal diffusion factor of the two isotopes (Severinghaus et al., 1998; Leuenberger et al., 1999), and it will only be significant if the seasonal variations of the firn temperature are considered. In this study, we did not incorporate the thermal diffusion into the model, because its effect was included in air mixing near the surface, which will be described later. Under such a simple condition, the time series of the atmospheric components can be easily converted into their vertical profiles in firn by using the age distribution. Therefore the atmospheric $\delta^{13}C$ values in the past were estimated inversely by the iterative procedure, which is equivalent to finding the continuous function that reproduces the vertical profile of $\delta^{13}C$ observed in firn.

### 3.1. *Age distribution*

The age distribution of $^{13}CO_2$ molecules in firn at Dome Fuji was calculated as a response function to a concentration pulse given at the surface of the ice sheet. This calculation was done for 1000 yr to obtain the age distribution of bubble air below the close-off zone as well, although the results for bubble air were not used in this study. The age distributions of $^{13}CO_2$, thus calculated, are shown in Fig. 5. The broadening of the age distribution is clearly seen for the open pore air, which is attributable to slow advection flow in the firn at Dome Fuji. The age distribution of bubble air also broadens rapidly with increasing depth in the close-off zone, and then slowly below that zone, due to the effects of the bubble trapping and the densification of ice occurring in the respective depth intervals. The age distribution calculated for $^{12}CO_2$ at each depth was apparently indistinguishable from that for $^{13}CO_2$, but $\delta^{13}C$ is differently defined even by such a small difference.

The mean age, derived by integrating the age distribution, gives a rough estimate of age for the open pore or bubble air. For a depth of 104 m at Dome Fuji, corresponding to just above the bottom of close-off zone, the mean age was calculated to be about 29 yr. The effective age for the air sampled at 103.7 m, defined as the age when the same $CO_2$ concentration value appeared in the atmosphere, was estimated to be about 22 yr, while its mean age was calculated to be about 26 yr from the age distribution of $^{12}CO_2$.

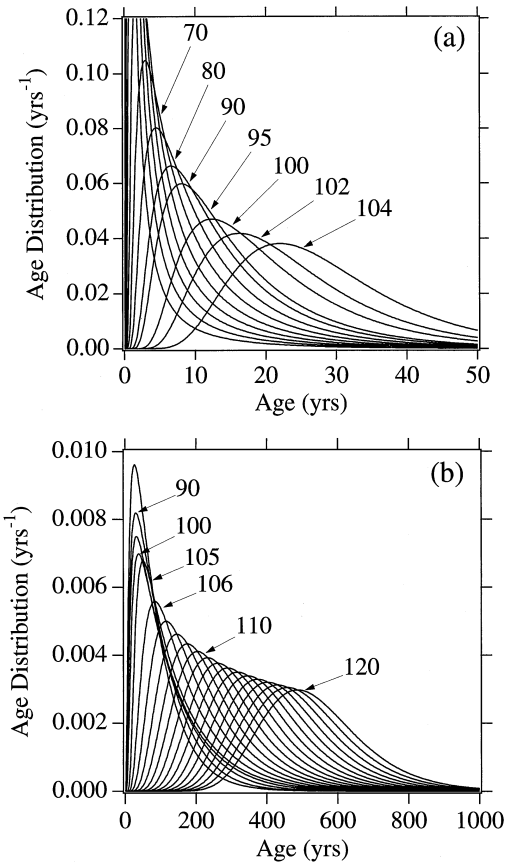


*Fig. 5.* Age distributions of $^{13}CO_2$ in (a) open pore and (b) bubble at selected depths (m) in firn at Dome Fuji. The actual calculation of the age distribution was made at 1 m intervals.

Figure 6 shows the ice ages and the mean ages of $CO_2$ molecule for the open pore and bubble air at Dome Fuji, which were calculated from the age distributions. The mean age of $CO_2$ in the bubble air was calculated to be about 140 yr at the bottom of the close-off zone, and increased rapidly with increasing depth below that zone, showing the same slope as the ice age. The age difference between the ice and $CO_2$ in the bubble air under the present firn condition was estimated to be about 2220 yr by simply subtracting 140 yr from the ice age of 2360 yr at the bottom of the close-off zone. This value is fairly consistent with the estimate of about 2200 yr which was made by Kawamura (2000) using the 'close-off depth', defined as the depth where half of air finally trapped in the ice is included (Schwander et al., 1988).

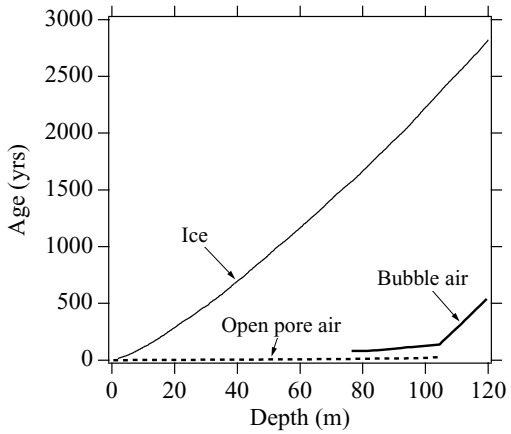


*Fig. 6.* Vertical profiles of the ice age (thin solid line) and the mean ages of $CO_2$ in bubble air (thick solid line) and open pore air (dashed line) at Dome Fuji.

### 3.2. *Reconstruction method*

As mentioned above, the past variation of the atmospheric $\delta^{13}$C was reconstructed inversely from its measured values in the firn at Dome Fuji, using an iterative procedure. In this process, the vertical distribution of $\delta^{13}$C in the firn was calculated from the concentrations of $^{12}CO_2$ and $^{13}CO_2$ that were independently obtained by using their assumed atmospheric histories. The vertical profile of the $CO_2$ concentration was already obtained for the derivation of the effective diffusivity, as described above. Therefore, the calculation was required only for $^{13}CO_2$. The concentration history of atmospheric $^{13}CO_2$ was calculated from the measured values of $\delta^{13}$C versus depth.

Before starting the iteration, the $\delta^{13}$C values observed in firn were rearranged into the time domain by calculating the mean ages from the age distributions of $^{13}CO_2$ at the respective depths, for use as a first guess of the atmospheric $\delta^{13}$C in the past. The iterative procedure consisted mainly of the following three steps. Firstly, the vertical profile of the $^{13}CO_2$ concentration in firn was calculated by using its age distributions and the first guess of the atmospheric $\delta^{13}$C variation history. Secondly, the profile of the $^{13}CO_2$ concentration thus calculated was compared with that fitted to the observed values, and then the differences between the calculated and observed $^{13}CO_2$ concentrations were obtained. At the same time, the vertical profile of $\delta^{13}$C was also calculated to compare with each observed value. Finally, the initially guessed values of the atmospheric $^{13}CO_2$ concentration were revised by slightly adjusting the respective values in proportion to the differences obtained in the second step. Here, it should be noted that the difference at each depth, $\Delta c_f(z)$, is caused by the atmospheric $^{13}CO_2$ value being assumed incorrectly to be in association not only with the mean age but also with the time interval defined by the age distribution. Therefore, the adjustment for the atmospheric $^{13}CO_2$ concentration, $\Delta c_a(t)$, was made proportional to the age distribution, $A(z,t)$

$$\Delta c_a(t) = \int \gamma(z) A(z,t) \Delta c_f(z)\, dz. \tag{14}$$

Here, $\gamma(z)$ is the weighting parameter, ranging between $-1$ and 0. This parameter was given at each layer so that $\Delta c_f(z)$ was weighted at the depths where the data were taken. These steps were repeated until the difference in $\delta^{13}$C obtained at the second step became less than 0.05‰.

The time period covered by this analysis spanned only about 30 yr before 1998. However, a longer record of the atmospheric $\delta^{13}$C is required for initializing the vertical profile of $\delta^{13}$C in firn. For this purpose, we used the $\delta^{13}$C data from the Law Dome ice core for the period 1700–1950 (Francey et al., 1999). The Law Dome data were connected smoothly with our initial guess of the atmospheric $\delta^{13}$C by using the spline fitting technique. The Law Dome data were not adjusted during the iterative calculation.

In this reconstruction process, the existence of a convective mixing zone near the surface should be considered. If the firn air is mixed with the atmosphere due to variations in temperature, pressure and wind stress at the surface, the age of the firn air becomes younger than that without such a mixing effect. Since no data at depths shallower than 10 m were available in this study, we cannot directly estimate the effect of the mixing zone on $\delta^{13}$C. However, from measurements of $\delta^{15}$N and $\delta^{18}$O in the firn air at Dome Fuji and H72, it was found that the mixing zone exists in the uppermost layer of firn at both sites, and that its mean thicknesses at the respective sites are 8–10 and 2–4 m (Kawamura, 2000). Taking this into account, we assumed in our model calculation that no diffusive transport occurred in the mixing zone, and that the $\delta^{13}$C values in the mixing zone varied in step with those in the atmosphere.

### 3.3. *Reconstruction test using the $CH_4$ data*

To check the validity of the analytical method developed in this study, we applied it to reconstruct the $CH_4$

concentration using the data obtained in firn at Dome Fuji. Details of the $CH_4$ concentration data used have been described elsewhere (Kawamura, 2000). Since systematic measurements of the atmospheric $CH_4$ concentration have been carried out in the Antarctic region since the 1980s (Aoki et al., 1992; Dlugokencky et al., 1994, 1998), the results reconstructed in this study can be compared directly with those of the direct observations. The effective diffusivity for the $CH_4$ molecule was obtained by multiplying that for $CO_2$ molecule by a factor of 1.291 (Trudinger et al., 1997). The data from the Law Dome ice core (Etheridge et al., 1998) were also used for the atmospheric $CH_4$ concentrations during the period 1700–1950, to initialize the vertical $CH_4$ distribution in firn. The $CH_4$ concentrations reconstructed from the Dome Fuji data are shown in Fig. 7, together with the results of the direct atmospheric measurements at the South Pole by NOAA/CMDL (available on their website, http://www.cmdl.noaa.gov/) and Syowa Station by NIPR and Tohoku University (our unpublished data). Both data sets were corrected for the difference between the concentration scales employed by NOAA/CMDL and NIPR-Tohoku University. As seen in this figure, the variations of the atmospheric $CH_4$ concentration estimated in this study are in good agreement with those from the direct measurements at the Antarctic stations. It is obvious that not only the monotonous $CH_4$ increase during the 1980s and 1990s, but also the lowering of the increasing trend during the 1990s, is reconstructed well by using the present method.

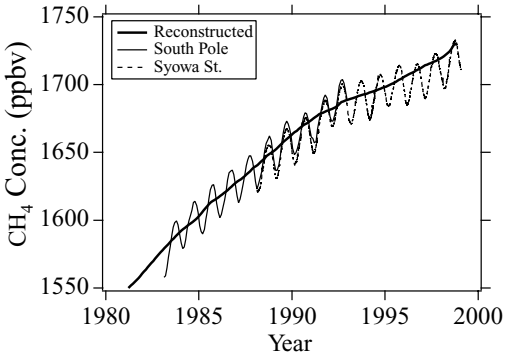


*Fig. 7.* Variations of the atmospheric $CH_4$ concentration reconstructed from its vertical profile observed in firn at Dome Fuji (thick solid line) and observed directly at the South Pole (thin line) and Syowa Station (dashed line).

## 4. Discussion

The $\delta^{13}C$ results obtained by applying the abovementioned procedure to the firn data at Dome Fuji are shown in Fig. 8. As seen from Fig. 8(a), the vertical profile of $\delta^{13}C$ calculated for firn at Dome Fuji is very consistent with the observational result. In general, the observed $\delta^{13}C$ value increases with depth, but its gradient is slightly gentler at depths between 50 and 70 m than at shallower than 50 m and becomes remarkably steep at the close-off zone around 100 m. The gentle gradient at 50–70 m yielded the stagnation in the reconstructed secular decrease of the atmospheric $\delta^{13}C$ for the period 1990–1995, as clearly seen in Fig. 8(b). In this connection, the mean ages of $^{13}CO_2$ obtained from its age distributions for the depths of 50–70 m

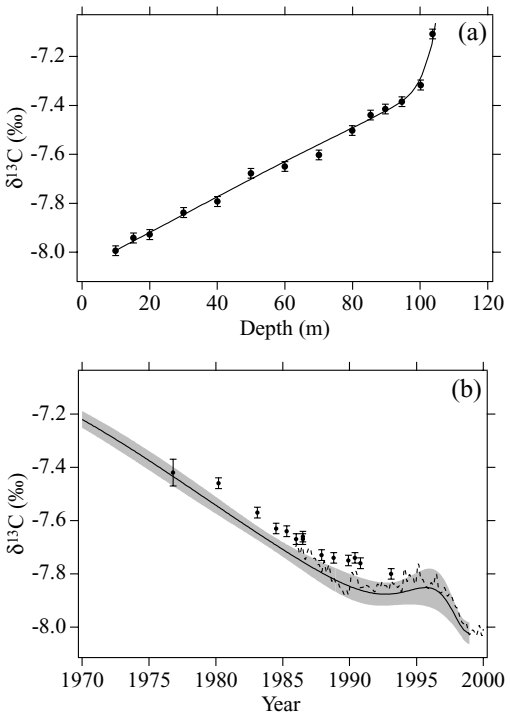


*Fig. 8.* (a) Vertical profiles of $\delta^{13}C$ observed (closed circles) and calculated (solid line) for firn at Dome Fuji, and (b) the atmospheric $\delta^{13}C$ variation reconstructed from its vertical profile in firn at Dome Fuji (solid line). The results of direct atmospheric measurements at Syowa Station and analyses of the Law Dome firn air are also plotted in panel (b) by a dashed line and closed circles, respectively. The uncertainties estimated for the reconstructed $\delta^{13}C$ variation are shown by shade.

were about 5–9 yr, which corresponds to the first half of the 1990s. The rapid increase of $\delta^{13}$C around 100 m is caused mainly by the small effective diffusivity at the close-off zone.

Since the atmospheric $\delta^{13}$C variations are reconstructed from the vertical profile of $\delta^{13}$C observed in firn, the uncertainty of the observed $\delta^{13}$C data and its propagation to the results through the iteration scheme should be considered carefully. Therefore, we examined the uncertainties of the atmospheric $\delta^{13}$C values reconstructed in this study, assuming simply that the errors of the $\delta^{13}$C values observed in firn at Dome Fuji were the same as the precision of our mass spectrometer analysis of 0.02‰ (1 standard deviation) (Nakazawa et al., 1997; Morimoto et al., 2000). The normal pseudo random numbers multiplied by 0.02 ‰ were first added to the $\delta^{13}$C values observed in firn, and then the same iteration method as above was applied to this hypothetical profile to obtain a new estimate of the atmospheric $\delta^{13}$C variation. This procedure was repeated for 1000 different sets of the random numbers, and the standard deviations of the reconstructed atmospheric $\delta^{13}$C variations were calculated. The standard deviations (1 $\sigma$), thus obtained, are also shown in Fig. 8(b). It is clearly seen that the standard deviations of the reconstructed atmospheric $\delta^{13}$C values are larger than that assumed for the observed $\delta^{13}$C values in firn. The maximum standard deviation amounted to about 0.074‰, which is more than three times as large as the uncertainty given to the observed $\delta^{13}$C values. This means that the error propagation plays an important role in essentially determining a confidence limit of our estimation. To reduce this uncertainty, precise analyses of $\delta^{13}$C of spatially finely sampled firn air are required.

The variations of the atmospheric $\delta^{13}$C derived in this study are compared in Fig. 8(b) with the results of the Law Dome firn analyses (Francey et al., 1999) and the direct atmospheric measurements at Syowa Station (Morimoto et al., 2001). Our results agree well with the observed values at Syowa Station, even for clear stagnation of the secular decrease and subsequent rapid decrease during the 1990s. A similar agreement was also found in the comparison to the atmospheric $\delta^{13}$C records at the South Pole (Keeling et al., 1995) and Cape Grim (Francey et al., 1999). The $\delta^{13}$C values at Syowa Station are slightly higher, by about 0.025‰ on average, than our best estimates. One possible cause of such a small difference may be attributable to the different geographical locations of Dome Fuji and Syowa Station; the Dome Fuji site is located on highland (3810 m a.s.l.) about 1000 km inland from Syowa Station. However, this difference is thought to be insignificant, because it is sufficiently smaller than the uncertainties of the present estimation. Since the same mass spectrometer and standard were used in this study and for the Syowa Station record, a fairly good agreement between both results demonstrates the effectiveness of our reconstruction method. Francey et al. (1999) also found a small difference, of 0.015 ‰ on average, between the $\delta^{13}$C values from the direct atmospheric measurements at Cape Grim and the analyses of the firn air at Law Dome, and they concluded such a difference to be insignificant.

The secular decreasing trend of the atmospheric $\delta^{13}$C derived in the present study is also in good agreement with that from the firn air at Law Dome. However, our retrieved $\delta^{13}$C values are systematically lower by 0.08 ‰, on average, than the values at Law Dome. This difference could be partly ascribed to the different isotopic analysis techniques used by the two laboratories involved.

To examine the validity of the atmospheric $\delta^{13}$C variation reconstructed from the data at Dome Fuji, we calculated the vertical distribution of $\delta^{13}$C for firn at H72 using it as a boundary condition to be given at the surface. The result shown in Fig. 9 is compared to the observed values. The calculated value of $\delta^{13}$C increases almost linearly with increasing depth at layers shallower than 40 m. This increasing trend becomes

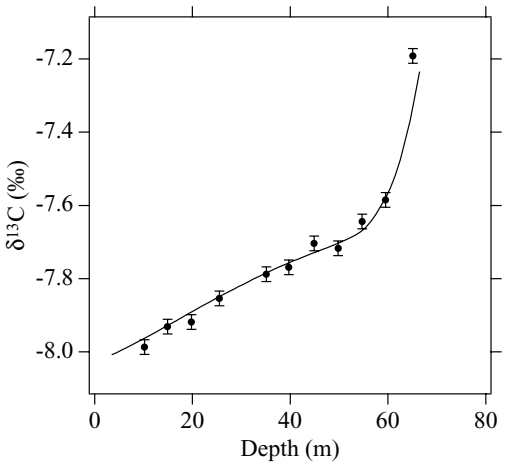


*Fig. 9.* Observed (closed circle) and calculated (solid line) vertical profiles of $\delta^{13}$C in firn at H72. The calculated values of $\delta^{13}$C were derived on the basis of the atmospheric $\delta^{13}$C variation reconstructed from the firn data at Dome Fuji.

slightly gentle in the 40–50 m layer, which is ascribed to the stagnation of the secular decrease of the atmospheric $\delta^{13}C$ in the early 1990s. The remarkable increase in $\delta^{13}C$ seen below 60 m is related to the non-diffusive layer existing at the lower half of the close-off zone. As mentioned before, the air in the open pore space of this layer moves down together with its surrounding firn. As shown in Fig. 1, the vertical speed of this layer of firn is about 0.42 m $yr^{-1}$. Therefore, the age difference between 60 and 66 m, corresponding to the top and the bottom of the non-diffusive layer, is calculated to be about 14 yr. The calculated values of $\delta^{13}C$ are in close agreement with the observed values, the differences between both values being less than 0.03‰, except for the data at 65 m. Considering the uncertainties in our $\delta^{13}C$ measurements, such small differences are insignificant.

## 5. Conclusions

The atmospheric $\delta^{13}C$ variation for the last few decades was reconstructed from the vertical distribution of $\delta^{13}C$ observed in firn at Dome Fuji, using a one-dimensional diffusion model. The validity of our analytical method and the results obtained was examined by comparing with the data from direct atmospheric measurements and analyses of the firn air at other sites. The results obtained from the present study are summarized as follows:

(1) A one-dimensional diffusion model was developed based on the theoretical formulation proposed by Schwander et al. (1993) and Rommelaere et al. (1997).

(2) The effective diffusivities in firn at Dome Fuji and H72 were estimated, so that the vertical $CO_2$ profile in firn was reproduced well by using the atmospheric $CO_2$ concentration history at the surface of ice sheet.

(3) An iteration method was developed for reconstructing the past variations of atmospheric components from their vertical profiles observed in firn. This method was verified by applying it to the $CH_4$ data, and the result obtained was found to be consistent with direct atmospheric measurements in the Antarctic region.

(4) The variation of the atmospheric $\delta^{13}C$ was reconstructed from the data observed in firn at Dome Fuji. Its temporal trend was in close agreement not only with those from the direct atmospheric measurements at Syowa Station, but also with those reconstructed from the firn air at Law Dome, although a small but systematic difference of $\delta^{13}C$ between Dome Fuji and Law Dome was found.

(5) The statistical error of the reconstructed values of the atmospheric $\delta^{13}C$ was investigated by using the normal pseudo-random numbers, and it was suggested that the uncertainties of the reconstructed atmospheric $\delta^{13}C$ values were larger than those of the $\delta^{13}C$ values observed in firn.

(6) The atmospheric $\delta^{13}C$ values reconstructed from the firn data at Dome Fuji were also supported by the fact that the vertical profile of $\delta^{13}C$ observed in firn at H72 agreed well with that calculated by giving them as a boundary condition at the surface of H72.

For a better understanding of the carbon cycle on the Earth's surface, combined analyses of the long-term variations of $CO_2$, its $\delta^{13}C$, and $O_2$ in the atmosphere are required (Keeling et al., 1996; Bender and Battle, 1999). The method developed in this study would contribute significantly to such analyses.

## 6. Acknowledgements

We are grateful to Dr. T. Yamada, Institute of Low Temperature Science, Hokkaido University, and Dr. K. Suzuki, Shinshu University, for collecting firn air at Dome Fuji and H72. We also thank Dr. Morimoto, NIPR, for providing us with the $\delta^{13}C$ data at Syowa Station.

## REFERENCES

Aoki, S., Nakazawa, T., Murayama, S. and Kawaguchi, S. 1992. Measurements of atmospheric methane at Japanese Antarctic Station, Syowa. *Tellus* **44B**, 273–281.

Battle, M., Bender, M., Sowers, T., Tans, P. P., Butler, J. H., Elkins, J. W., Ellis, J. T., Conway, T., Zhang, N., Lang, P. and Clarke, A. D. 1996. Atmospheric gas concentrations over the past century measured in air from firn at the South Pole. *Nature* **383**, 231–235.

Bender, M. and Battle, M. 1999. Carbon cycle studies based on the distribution of $O_2$ in air. *Tellus* **51B**, 165–169.

Crank, J. 1975. *The Mathematics of Diffusion*. Clarendon, Oxford, 414 pp.

Dlugokencky, E. J., Steele, L. P., Lang, P. M. and Masarie K. A. 1994. The growth rate and distribution of atmospheric methane. *J. Geophys. Res.* **99**, 17 021–17 043.

Dlugokencky, E. J., Masarie, K. A., Lang, P. M. and Tans, P. P. 1998. Continuing decline in the growth rate of the atmospheric methane burden. *Nature* **393**, 447–450.

Etheridge, D. M., Steele, L. P., Francey, R. J. and Langenfelds, R. L. 1998. Atmospheric methane between 1000 A.D. and present: evidence of anthropogenic emissions and climatic variability. *J. Geophys. Res.* **103**, 15 979–15 994.

Francey, R. J., Robbins, F. J., Allison, C. E. and Richards, N. G. 1990. The CSIRO global survey of CO2 stable isotopes. In: *Baseline Atmospheric Program* (Australia) *1988*, (eds. S. R. Wilson and G. P. Ayers), Department of Administrative Service/Bureau of Meteorology in cooperation with CSIRO Division of Atmospheric Research Cape Grim BAPS, Tasmania, Australia, 16–27.

Francey, R. J., Allison, C. E., Etheridge, D. M., Trudinger, C. M., Enting, I. G., Leuenberger, M., Langenfelds, R. L., Michel, E. and Steele, P. L. 1999. A 1000-year high precision record of $\delta^{13}C$ in atmospheric $CO_2$. *Tellus* **51B**, 170–193.

Friedli, H., Siegenthaler, U., Rauber, D. and Oeschger, H. 1987. Measurements of concentration, $^{13}C/^{12}C$ and $^{18}O/^{16}O$ ratios of tropospheric carbon dioxide over Switzerland. *Tellus* **39B**, 80–88.

Hirsch, C. 1988. Thomas algorithm for tridiagonal systems. In: *Numerical Computation of Internal and External Flows*. Willey, Chichester, Vol. 1, pp. 505–508.

Kawamura, K. 2000. Variations of atmospheric components over the past 340, 000 yr from Dome Fuji deep ice core, Antarctica, Ph.D. Thesis, Tohoku University, Sendai, Japan.

Kawamura, K., Nakazawa, T., Machida, T., Morimoto, S., Aoki, S., Ishizawa, M., Fujii, Y. and Watanabe, O. 2000. Variations of the carbon isotopic ratio in atmospheric $CO_2$ over the last 250 yr recorded in an ice core from H15, Antarctica. *Polar Meteorol. Glaciol.* **14**, 47–57.

Keeling, C. D., Bacastow, R. B., Carter, A. F., Piper, S. C., Whorf, T. P., Heimann, M., Mook, W. G. and Roeloffzen, H. 1989. A three-dimensional model of atmospheric $CO_2$ transport based on observed winds: 1. Analysis of observed data. *AGU Monograph* **55**, Washington, American Geophysical Union, 165–236.

Keeling, C. D., Whorf, T. P., Wahlen, M. and van der Plicht, J. 1995. Interannual extremes in the rate of rise of atmospheric carbon dioxide since 1980, *Nature* **375**, 666–670.

Keeling, R. F., Piper, S. C. and Heimann, M. 1996. Global and hemispheric $CO_2$ sinks deduced from changes in atmospheric $O_2$ concentration. *Nature* **381**, 218–221.

Leuenberger, M. C., Lang, C. and Schwander, J. 1999. Delta$^{15}$N measurements as a calibration tool for the paleothermometer and gas-ice age differences: a case study for the 8200 B.P. event on GRIP ice. *J. Geophys. Res.* **104**, 22163–22170.

Morimoto, S., Nakazawa, T., Higuchi, K. and Aoki, S. 2000. Latitudinal distribution of atmospheric $CO_2$ sources and sinks inferred by $\delta^{13}C$ measurements from 1985 to 1991. *J. Geophys. Res.* **105**, 24 315–24 326.

Morimoto, S., Nakazawa, T., Aoki, S., Hashida, G. and Yamanouchi, T. 2001. Temporal variations of the atmospheric $CO_2$ concentration and isotope ratios observed at Syowa Station, Antarctica, since 1984. In: *Sixth International Carbon Dioxide Conference, Extended Abstract,* **1**, 205–207.

Nakazawa, T., Morimoto, S., Aoki, S. and Tanaka, M. 1993a. Time and space variations of the carbon isotopic ratio of tropospheric carbon dioxide over Japan. *Tellus* **45B**, 258–274.

Nakazawa, T., Machida, T., Tanaka, M., Fujii, Y., Aoki, S. and Watanabe, O. 1993b. Atmospheric $CO_2$ concentrations and carbon isotopic ratios for the last 250 yr deduced from an Antarctic ice core, H15. In: *Extended Abstracts of the 4th International $CO_2$ Conference, Carqueiranne*, France, 13–17 September 1993. World Meteorological Organization, WMO/TD-NO 561.

Nakazawa, T., Morimoto S., Aoki S. and Tanaka M. 1997. Temporal and spatial variations of the carbon isotopic ratio of atmospheric carbon dioxide in the western Pacific region. *J. Geophys, Res*. **102**, 1271–1285.

Rommelaere, V., Arnaud, L. and Barnola, J. M. 1997. Reconstructing recent atmospheric trace gas concentrations from polar firn and bubbly ice data by inverse methods. *J. Geophys. Res.* **102**, 30 069–30 083.

Schwander, J., 1989. The transformation of snow to ice and the occlusion of gases. In: *The Environmental Record in Glaciers and Ice Sheets* (eds. H. Oeschger and C. C. Langway), John Wiley & Sons, Berlin 53–67.

Schwander, J., Stauffer, B. and Sigg, A. 1988. Air mixing in firn and the air at pore close-off. *Ann. Glaciol*. **10**, 141–145.

Schwander, J., Barnola, J. M., Andrie, C., Leuenberger, M., Ludin, A., Raynaud, D. and Stauffer, B. 1993. The age of the air in the firn and the ice at Summit, Greenland. *J. Geophys. Res.* **98**, 2831–2838.

Severinghaus, J. P., Sowers, T., Brook, E. J., Alley, R. B. and Bender, M. L. 1998. Timing of abrupt climate change at the end of the Younger Dryas interval from thermally fractionated gases in polar ice. *Nature* **391**, 141–146.

Siegenthaler, U. and Münnich, K. O. 1981. $^{13}C/^{12}C$ fractionation during $CO_2$ transfer from air to sea. In: *Carbon Cycle Modeling* (ed. B. Bolin), John Wiley, New York, 246–257.

Sowers, T., Bender, M., Raynaud, D. and Korotkevich, Y. S. 1992. $\delta^{15}N$ of $N_2$ in air trapped in polar ice: a tracer of gas transport in the firn and a possible constraint on ice age-gas age differences. *J. Geophys. Res.* **97**, 15 683–15 697.

Trolier, M., White, J. W. C., Tans, P. P., Masarie, K. A. and Gemery, P. A. 1996. Monitoring the isotopic composition of atmospheric $CO_2$: Measurements from the NOAA Global Air Sampling Network. *J. Geophys. Res.* **101**, 25 897–25 916.

Trudinger, C. M., Enting, I. G., Etheridge, D. M., Francey, R. J., Levchenko, V. A., Steele, L. P., Raynaud, D. and Arnaud, L. 1997. Modeling air movement and bubble trapping in firn. *J. Geophys. Res.* **102**, 6747–6763.